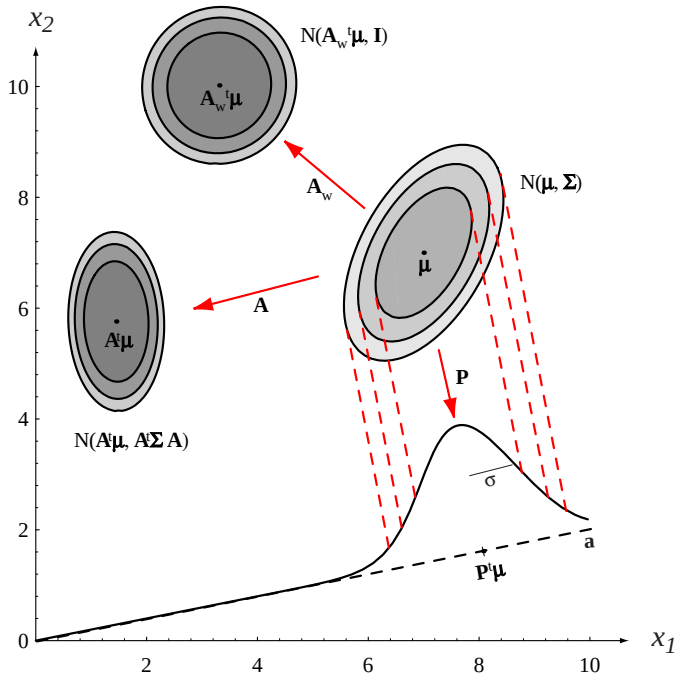

Figure 2.8: The action of a linear transformation on the feature space will convert an arbitrary normal distribution into another normal distribution. One transformation, $\mathbf{A}$, takes the source distribution into distribution $N(\mathbf{A}^t\boldsymbol{\mu}, \mathbf{A}^t\boldsymbol{\Sigma}\mathbf{A})$. Another linear transformation — a projection $\mathbf{P}$ onto line $\mathbf{a}$ — leads to $N(\mu, \sigma^2)$ measured along $\mathbf{a}$. While the transforms yield distributions in a different space, we show them superimposed on the original $x_1 - x_2$ space. A whitening transform leads to a circularly symmetric Gaussian, here shown displaced.

2.6 Discriminant Functions for the Normal Density

In Sect. 2.4.1 we saw that the minimum-error-rate classification can be achieved by use of the discriminant functions

$$g_i(\mathbf{x}) = \ln\, p(\mathbf{x}|\omega_i) + \ln\, P(\omega_i). \tag{46}$$

This expression can be readily evaluated if the densities $p(\mathbf{x}|\omega_i)$ are multivariate normal, i.e., if $p(\mathbf{x}|\omega_i) \sim N(\boldsymbol{\mu}_i, \boldsymbol{\Sigma}_i)$. In this case, then, from Eq. 37 we have

$$g_i(\mathbf{x}) = -\frac{1}{2}(\mathbf{x} - \boldsymbol{\mu}_i)^t \boldsymbol{\Sigma}_i^{-1}(\mathbf{x} - \boldsymbol{\mu}_i) - \frac{d}{2}\ln 2\pi - \frac{1}{2}\ln |\boldsymbol{\Sigma}_i| + \ln\, P(\omega_i). \tag{47}$$

Let us examine the discriminant function and resulting classification for a number of special cases.

2.6.1 Case 1: $\boldsymbol{\Sigma}_i = \sigma^2\mathbf{I}$

The simplest case occurs when the features are statistically independent, and when each feature has the same variance, σ^2. In this case the covariance matrix is diagonal,

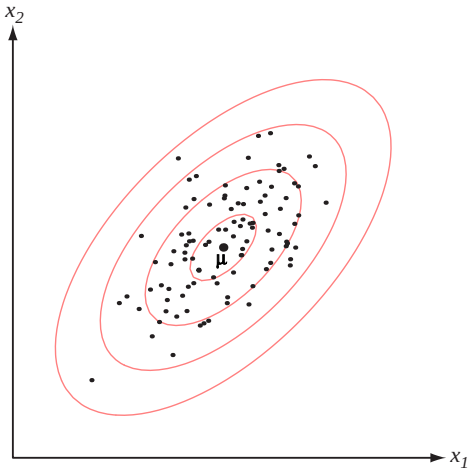

Figure 2.9: Samples drawn from a two-dimensional Gaussian lie in a cloud centered on the mean $\boldsymbol{\mu}$. The red ellipses show lines of equal probability density of the Gaussian.

being merely σ^2 times the identity matrix $\mathbf{I}$. Geometrically, this corresponds to the situation in which the samples fall in equal-size hyperspherical clusters, the cluster for the ith class being centered about the mean vector $\boldsymbol{\mu}_i$. The computation of the determinant and the inverse of $\boldsymbol{\Sigma}_i$ is particularly easy: $|\boldsymbol{\Sigma}_i| = \sigma^{2d}$ and $\boldsymbol{\Sigma}_i^{-1} = (1/\sigma^2)\mathbf{I}$. Since both $|\boldsymbol{\Sigma}_i|$ and the $(d/2)\ \ln\ 2\pi$ term in Eq. 47 are independent of i, they are unimportant additive constants that can be ignored. Thus we obtain the simple discriminant functions

$$g_i(\mathbf{x}) = -\frac{\|\mathbf{x} - \boldsymbol{\mu}_i\|^2}{2\sigma^2} + \ln\ P(\omega_i), \tag{48}$$

EUCLIDEAN NORM

where $\|\cdot\|$ is the *Euclidean norm*, that is,

$$\|\mathbf{x} - \boldsymbol{\mu}_i\|^2 = (\mathbf{x} - \boldsymbol{\mu}_i)^t(\mathbf{x} - \boldsymbol{\mu}_i). \tag{49}$$

If the prior probabilities are not equal, then Eq. 48 shows that the squared distance $\|\mathbf{x} - \boldsymbol{\mu}\|^2$ must be normalized by the variance σ^2 and offset by adding $\ln\ P(\omega_i)$; thus, if $\mathbf{x}$ is equally near two different mean vectors, the optimal decision will favor the a priori more likely category.

Regardless of whether the prior probabilities are equal or not, it is not actually necessary to compute distances. Expansion of the quadratic form $(\mathbf{x} - \boldsymbol{\mu}_i)^t(\mathbf{x} - \boldsymbol{\mu}_i)$ yields

$$g_i(\mathbf{x}) = -\frac{1}{2\sigma^2}[\mathbf{x}^t\mathbf{x} - 2\boldsymbol{\mu}_i^t\mathbf{x} + \boldsymbol{\mu}_i^t\boldsymbol{\mu}_i] + \ln\ P(\omega_i), \tag{50}$$

which appears to be a quadratic function of $\mathbf{x}$. However, the quadratic term $\mathbf{x}^t\mathbf{x}$ is the same for all i, making it an ignorable additive constant. Thus, we obtain the equivalent *linear discriminant functions*

LINEAR DISCRIMINANT

$$g_i(\mathbf{x}) = \mathbf{w}_i^t\mathbf{x} + w_{i0}, \tag{51}$$

where

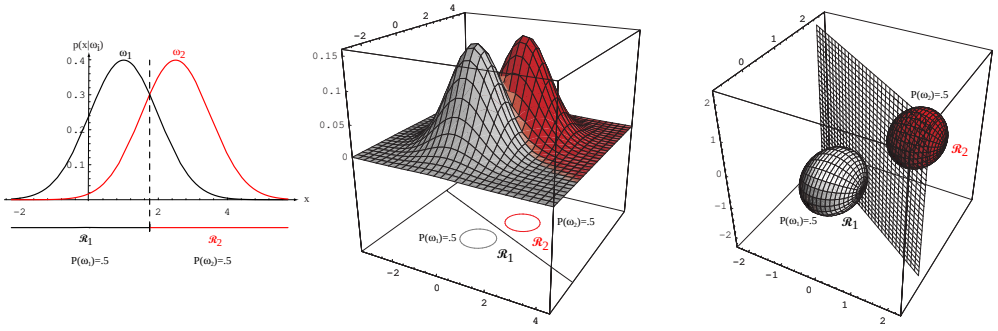

Figure 2.10: If the covariances of two distributions are equal and proportional to the identity matrix, then the distributions are spherical in d dimensions, and the boundary is a generalized hyperplane of $d-1$ dimensions, perpendicular to the line separating the means. In these 1-, 2-, and 3-dimensional examples, we indicate $p(\mathbf{x}|\omega_i)$ and the boundaries for the case $P(\omega_1) = P(\omega_2)$. In the 3-dimensional case, the grid plane separates $\mathcal{R}_1$ from $\mathcal{R}_2$.

$$\mathbf{w}_i = \frac{1}{\sigma^2}\boldsymbol{\mu}_i \tag{52}$$

and

$$w_{i0} = \frac{-1}{2\sigma^2}\boldsymbol{\mu}_i^t\boldsymbol{\mu}_i + \ln\, P(\omega_i). \tag{53}$$

We call w_{i0} the *threshold* or *bias* in the ith direction.

THRESHOLD

BIAS

A classifier that uses linear discriminant functions is called a *linear machine*. This kind of classifier has many interesting theoretical properties, some of which will be discussed in detail in Chap. **??**. At this point we merely note that the decision surfaces for a linear machine are pieces of hyperplanes defined by the linear equations $g_i(\mathbf{x}) = g_j(\mathbf{x})$ for the two categories with the highest posterior probabilities. For our particular case, this equation can be written as

LINEAR MACHINE

$$\mathbf{w}^t(\mathbf{x} - \mathbf{x}_0) = 0, \tag{54}$$

where

$$\mathbf{w} = \boldsymbol{\mu}_i - \boldsymbol{\mu}_j \tag{55}$$

and

$$\mathbf{x}_0 = \frac{1}{2}(\boldsymbol{\mu}_i + \boldsymbol{\mu}_j) - \frac{\sigma^2}{\|\boldsymbol{\mu}_i - \boldsymbol{\mu}_j\|^2}\ln\frac{P(\omega_i)}{P(\omega_j)}(\boldsymbol{\mu}_i - \boldsymbol{\mu}_j). \tag{56}$$

This equation defines a hyperplane through the point $\mathbf{x}_0$ and orthogonal to the vector $\mathbf{w}$. Since $\mathbf{w} = \boldsymbol{\mu}_i - \boldsymbol{\mu}_j$, the hyperplane separating $\mathcal{R}_i$ and $\mathcal{R}_j$ is orthogonal to the line linking the means. If $P(\omega_i) = P(\omega_j)$, the second term on the right of Eq. 56 vanishes, and thus the point $\mathbf{x}_0$ is halfway between the means, and the hyperplane is the perpendicular bisector of the line between the means (Fig. 2.11). If $P(\omega_i) \neq P(\omega_j)$, the point $\mathbf{x}_0$ shifts away from the more likely mean. Note, however, that if the variance

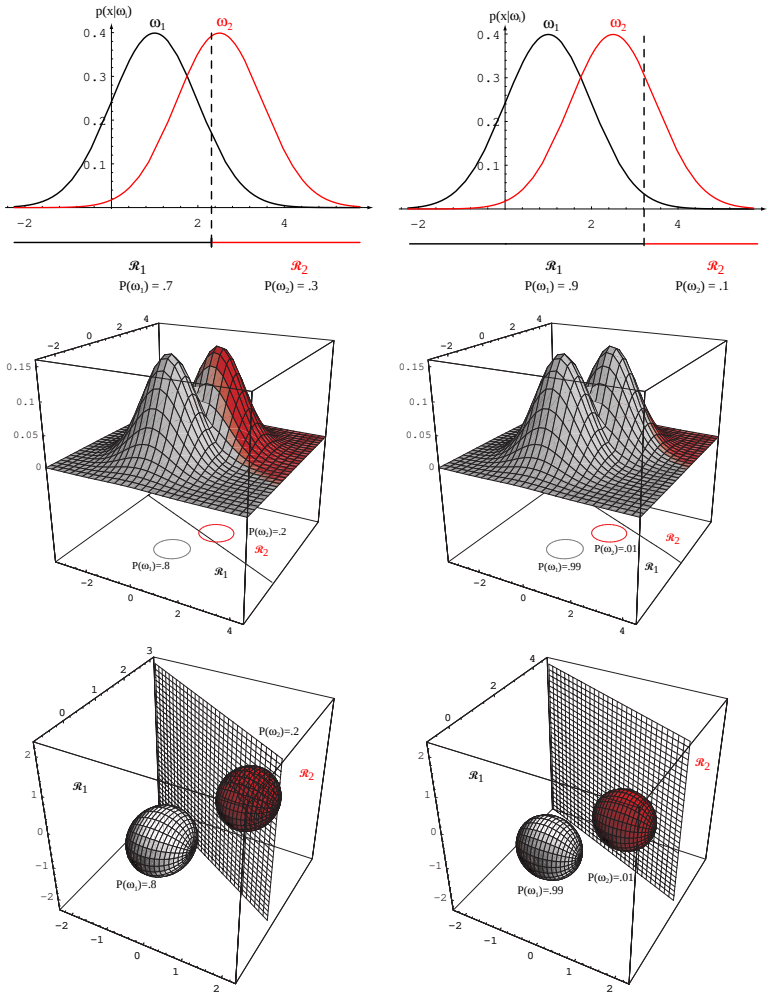

Figure 2.11: As the priors are changed, the decision boundary shifts; for sufficiently disparate priors the boundary will not lie between the means of these 1-, 2- and 3-dimensional spherical Gaussian distributions.

σ^2 is small relative to the squared distance $\|\boldsymbol{\mu}_i - \boldsymbol{\mu}_j\|$, then the position of the decision boundary is relatively insensitive to the exact values of the prior probabilities.

If the prior probabilities $P(\omega_i)$ are the same for all c classes, then the ln $P(\omega_i)$ term becomes another unimportant additive constant that can be ignored. When this happens, the optimum decision rule can be stated very simply: to classify a feature vector $\mathbf{x}$, measure the Euclidean distance $\|\mathbf{x} - \boldsymbol{\mu}_i\|$ from each $\mathbf{x}$ to each of the c mean vectors, and assign $\mathbf{x}$ to the category of the nearest mean. Such a classifier is called a *minimum distance classifier*. If each mean vector is thought of as being an ideal prototype or template for patterns in its class, then this is essentially a *template-matching* procedure (Fig. 2.10), a technique we will consider again in Chap. **??** Sect. **??** on the nearest-neighbor algorithm.

MINIMUM DISTANCE CLASSIFIER

TEMPLATE-MATCHING

2.6.2 Case 2: $\boldsymbol{\Sigma}_i = \boldsymbol{\Sigma}$

Another simple case arises when the covariance matrices for all of the classes are identical but otherwise arbitrary. Geometrically, this corresponds to the situation in which the samples fall in hyperellipsoidal clusters of equal size and shape, the cluster for the ith class being centered about the mean vector $\boldsymbol{\mu}_i$. Since both $|\boldsymbol{\Sigma}_i|$ and the $(d/2)\ \ln 2\pi$ term in Eq. 47 are independent of i, they can be ignored as superfluous additive constants. This simplification leads to the discriminant functions

$$g_i(\mathbf{x}) = -\frac{1}{2}(\mathbf{x} - \boldsymbol{\mu}_i)^t \boldsymbol{\Sigma}^{-1}(\mathbf{x} - \boldsymbol{\mu}_i) + \ln\ P(\omega_i). \tag{57}$$

If the prior probabilities $P(\omega_i)$ are the same for all c classes, then the $\ln\ P(\omega_i)$ term can be ignored. In this case, the optimal decision rule can once again be stated very simply: to classify a feature vector $\mathbf{x}$, measure the squared Mahalanobis distance $(\mathbf{x} - \boldsymbol{\mu}_i)^t \boldsymbol{\Sigma}^{-1}(\mathbf{x} - \boldsymbol{\mu}_i)$ from $\mathbf{x}$ to each of the c mean vectors, and assign $\mathbf{x}$ to the category of the nearest mean. As before, unequal prior probabilities bias the decision in favor of the a priori more likely category.

Expansion of the quadratic form $(\mathbf{x} - \boldsymbol{\mu}_i)^t \boldsymbol{\Sigma}^{-1}(\mathbf{x} - \boldsymbol{\mu}_i)$ results in a sum involving a quadratic term $\mathbf{x}^t \boldsymbol{\Sigma}^{-1} \mathbf{x}$ which here is independent of i. After this term is dropped from Eq. 57, the resulting discriminant functions are again linear:

$$g_i(\mathbf{x}) = \mathbf{w}_i^t \mathbf{x} + w_{i0}, \tag{58}$$

where

$$\mathbf{w}_i = \boldsymbol{\Sigma}^{-1} \boldsymbol{\mu}_i \tag{59}$$

and

$$w_{i0} = -\frac{1}{2} \boldsymbol{\mu}_i^t \boldsymbol{\Sigma}^{-1} \boldsymbol{\mu}_i + \ln\ P(\omega_i). \tag{60}$$

Since the discriminants are linear, the resulting decision boundaries are again hyperplanes (Fig. 2.10). If $\mathcal{R}_i$ and $\mathcal{R}_j$ are contiguous, the boundary between them has the equation

$$\mathbf{w}^t(\mathbf{x} - \mathbf{x}_0) = 0, \tag{61}$$

where

$$\mathbf{w} = \boldsymbol{\Sigma}^{-1}(\boldsymbol{\mu}_i - \boldsymbol{\mu}_j) \tag{62}$$

and

$$\mathbf{x}_0 = \frac{1}{2}(\boldsymbol{\mu}_i + \boldsymbol{\mu}_j) - \frac{\ln\ [P(\omega_i)/P(\omega_j)]}{(\boldsymbol{\mu}_i - \boldsymbol{\mu}_j)^t \boldsymbol{\Sigma}^{-1}(\boldsymbol{\mu}_i - \boldsymbol{\mu}_j)}(\boldsymbol{\mu}_i - \boldsymbol{\mu}_j). \tag{63}$$

Since $\mathbf{w} = \boldsymbol{\Sigma}^{-1}(\boldsymbol{\mu}_i - \boldsymbol{\mu}_j)$ is generally not in the direction of $\boldsymbol{\mu}_i - \boldsymbol{\mu}_j$, the hyperplane separating $\mathcal{R}_i$ and $\mathcal{R}_j$ is generally not orthogonal to the line between the means. However, it does intersect that line at the point $\mathbf{x}_0$ which is halfway between the means if the prior probabilities are equal. If the prior probabilities are not equal, the optimal boundary hyperplane is shifted away from the more likely mean (Fig. 2.12). As before, with sufficient bias the decision plane need not lie between the two mean vectors.

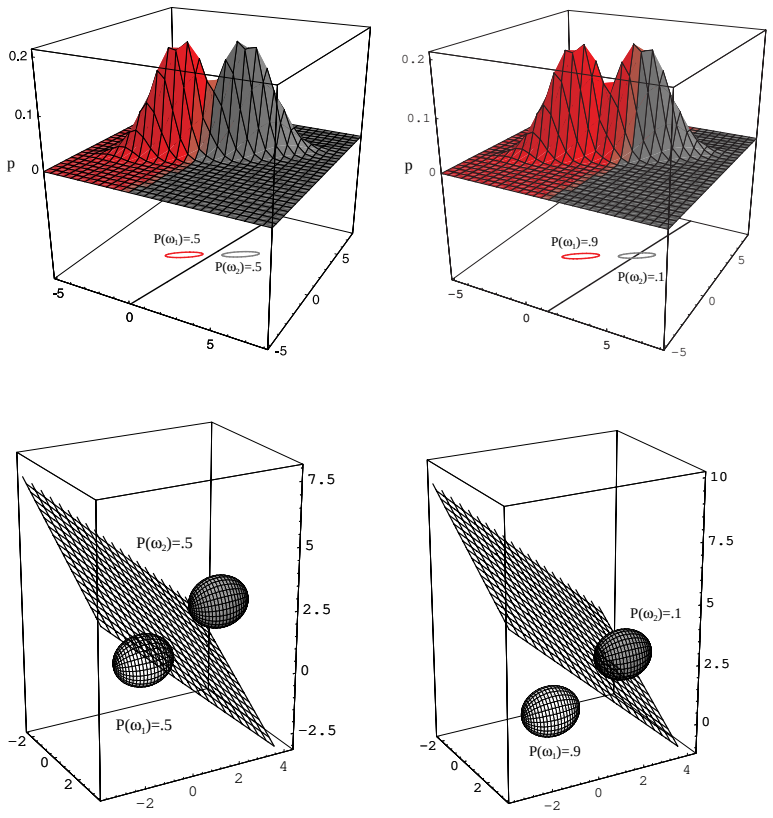

Figure 2.12: Probability densities (indicated by the surfaces in two dimensions and ellipsoidal surfaces in three dimensions) and decision regions for equal but asymmetric Gaussian distributions. The decision hyperplanes need not be perpendicular to the line connecting the means.

2.6.3 Case 3: $\boldsymbol{\Sigma}_i$ = arbitrary

In the general multivariate normal case, the covariance matrices are different for each category. The only term that can be dropped from Eq. 47 is the $(d/2)\ln 2\pi$ term, and the resulting discriminant functions are inherently quadratic:

$$g_i(\mathbf{x}) = \mathbf{x}^t\mathbf{W}_i\mathbf{x} + \mathbf{w}_i^t\mathbf{x} + w_{i0}, \tag{64}$$

where

$$\mathbf{W}_i = -\frac{1}{2}\boldsymbol{\Sigma}_i^{-1}, \tag{65}$$

$$\mathbf{w}_i = \boldsymbol{\Sigma}_i^{-1}\boldsymbol{\mu}_i \tag{66}$$

and

$$w_{i0} = -\frac{1}{2}\boldsymbol{\mu}_i^t\boldsymbol{\Sigma}_i^{-1}\boldsymbol{\mu}_i - \frac{1}{2}\ln|\boldsymbol{\Sigma}_i| + \ln P(\omega_i). \tag{67}$$

HYPER-QUADRIC

The decision surfaces are *hyperquadrics*, and can assume any of the general forms — hyperplanes, pairs of hyperplanes, hyperspheres, hyperellipsoids, hyperparaboloids, and hyperhyperboloids of various types (Problem 29). Even in one dimension, for arbitrary covariance the decision regions need not be simply connected (Fig. 2.13). The two- and three-dimensional examples in Fig. 2.14 & 2.15 indicate how these different forms can arise. These variances are indicated by the contours of constant probability density.

The extension of these results to more than two categories is straightforward though we need to keep clear which two of the total c categories are responsible for any boundary segment. Figure 2.16 shows the decision surfaces for a four-category case made up of Gaussian distributions. Of course, if the distributions are more complicated, the decision regions can be even more complex, though the same underlying theory holds there too.

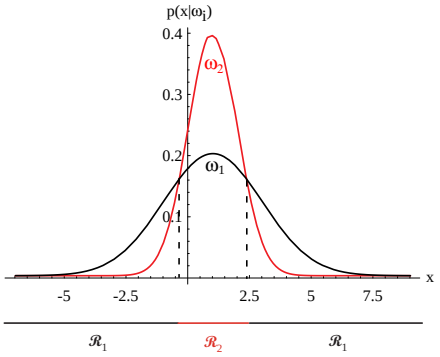

Figure 2.13: Non-simply connected decision regions can arise in one dimensions for Gaussians having unequal variance.

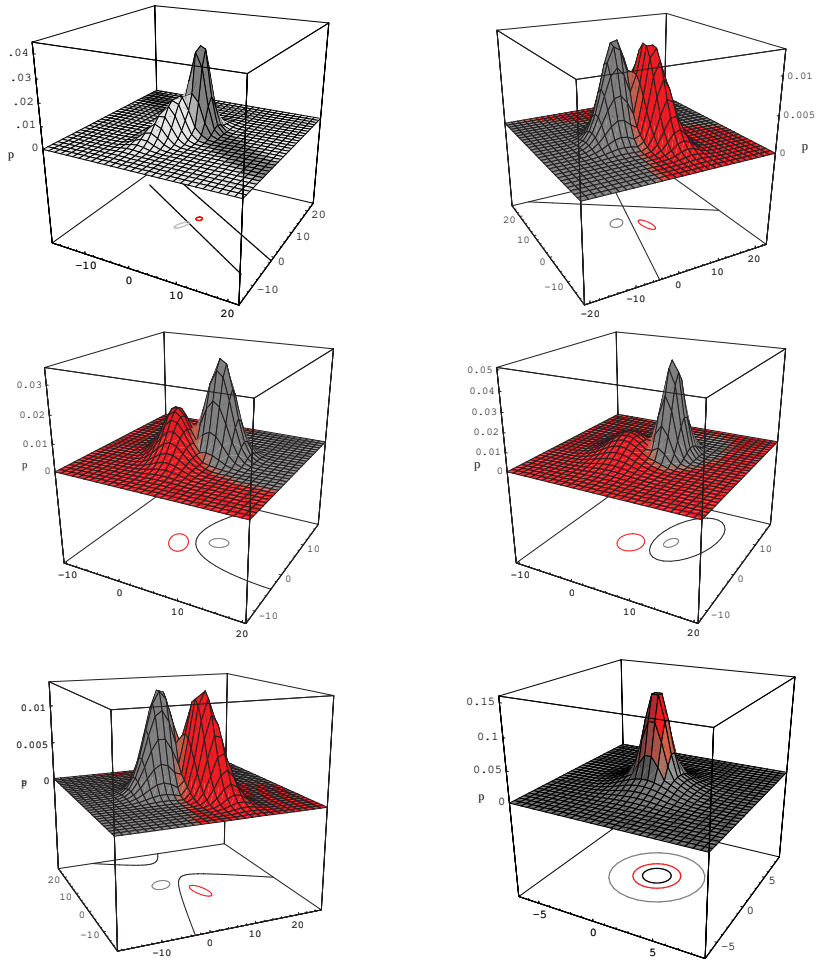

Figure 2.14: Arbitrary Gaussian distributions lead to Bayes decision boundaries that are general hyperquadrics. Conversely, given any hyperquadratic, one can find two Gaussian distributions whose Bayes decision boundary is that hyperquadric.

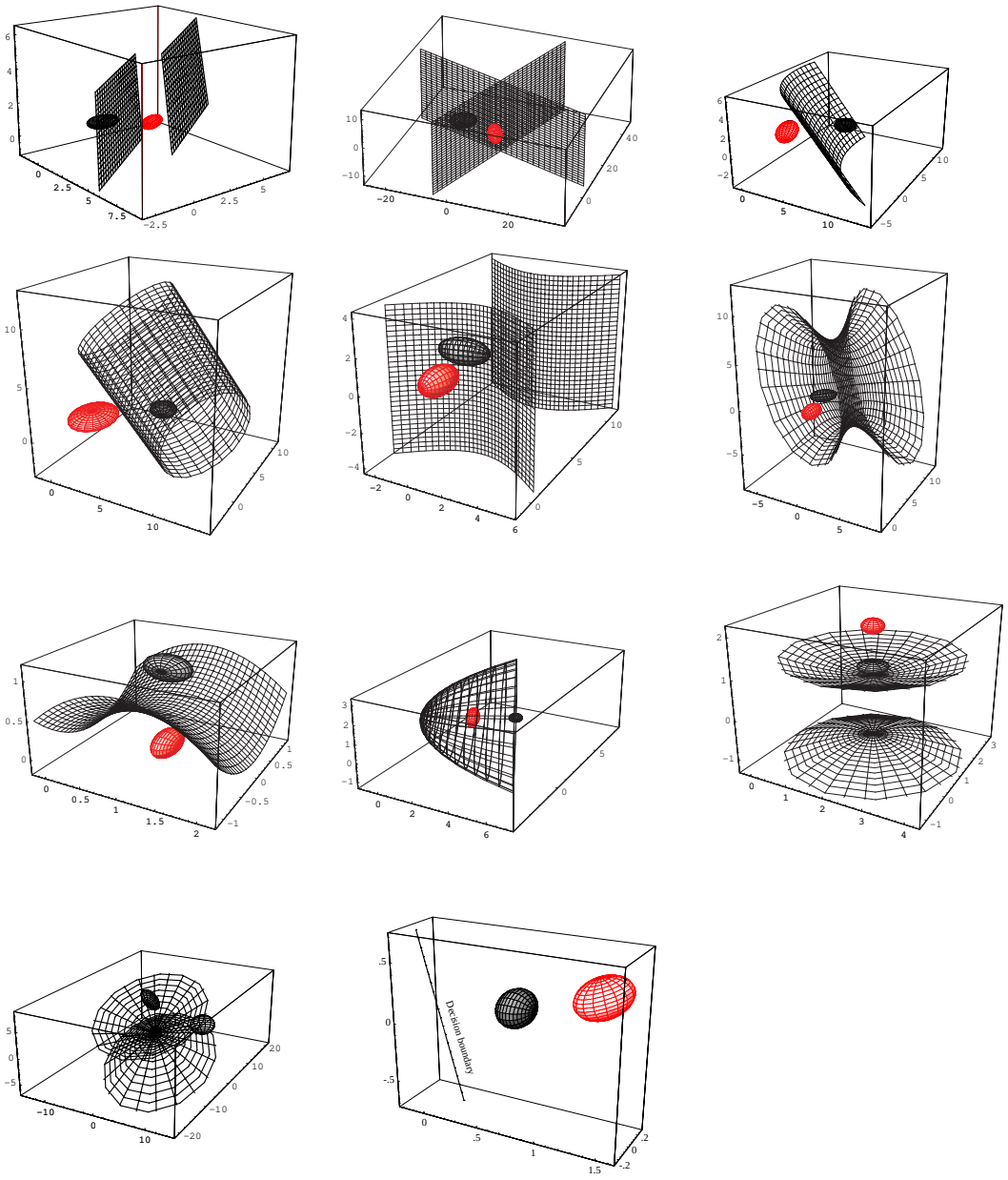

Figure 2.15: Arbitrary three-dimensional Gaussian distributions yield Bayes decision boundaries that are two-dimensional hyperquadrics. There are even degenerate cases in which the decision boundary is a line.

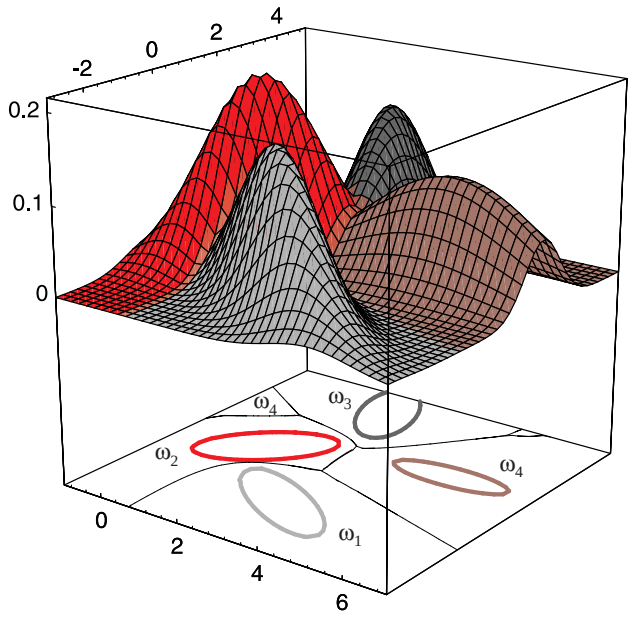

Figure 2.16: The decision regions for four normal distributions. Even with such a low number of categories, the shapes of the boundary regions can be rather complex.

Example 1: Decision regions for two-dimensional Gaussian data

To clarify these ideas, we explicitly calculate the decision boundary for the two-category two-dimensional data in the Example figure. Let ω_1 be the set of the four black points, and ω_2 the red points. Although we will spend much of the next chapter understanding how to estimate the parameters of our distributions, for now we simply assume that we need merely calculate the means and covariances by the discrete versions of Eqs. 39 & 40; they are found to be:

$$\boldsymbol{\mu}_1 = \begin{bmatrix} 3 \\ 6 \end{bmatrix}; \quad \boldsymbol{\Sigma}_1 = \begin{pmatrix} 1/2 & 0 \\ 0 & 2 \end{pmatrix} \text{ and } \boldsymbol{\mu}_2 = \begin{bmatrix} 3 \\ -2 \end{bmatrix}; \quad \boldsymbol{\Sigma}_2 = \begin{pmatrix} 2 & 0 \\ 0 & 2 \end{pmatrix}.$$

The inverse matrices are then,

$$\boldsymbol{\Sigma}_1^{-1} = \begin{pmatrix} 2 & 0 \\ 0 & 1/2 \end{pmatrix} \quad \text{and} \quad \boldsymbol{\Sigma}_2^{-1} = \begin{pmatrix} 1/2 & 0 \\ 0 & 1/2 \end{pmatrix}.$$

We assume equal prior probabilities, $P(\omega_1) = P(\omega_2) = 0.5$, and substitute these into the general form for a discriminant, Eqs. 64 – 67, setting $g_1(\mathbf{x}) = g_2(\mathbf{x})$ to obtain the decision boundary:

$$x_2 = 3.514 - 1.125x_1 + 0.1875x_1^2.$$

This equation describes a parabola with vertex at $\binom{3}{1.83}$. Note that despite the fact that the variance in the data along the x_2 direction for both distributions is the same, the decision boundary does not pass through the point $\binom{3}{2}$, midway between the means, as we might have naively guessed. This is because for the ω_1 distribution, the probability distribution is "squeezed" in the x_1-direction more so than for the ω_2 distribution. Because the overall prior probabilities are the same (i.e., the integral over space of the probability density), the distribution is increased along the x_2 direction (relative to that for the ω_2 distribution). Thus the decision boundary lies slightly lower than the point midway between the two means, as can be seen in the decision boundary.

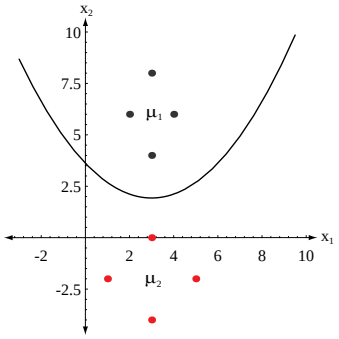

The computed Bayes decision boundary for two Gaussian distributions, each based on four data points.